Available online at www.sciencedirect.com
ScienceDirect
Journal of Molecular Spectroscopy 240 (2006) 238–243
Journal of MOLECULAR SPECTROSCOPY
www.elsevier.com/locate/jms

Optical–optical double resonance spectroscopy of the $\tilde{D}^2\Sigma^+$–$\tilde{A}^2\Pi$ transition of CaOH

M.J. Dick [a], P.M. Sheridan [b,1], J.-G. Wang [b], S. Yu [b], P.F. Bernath [a,b,*]

[a] Department of Physics, University of Waterloo, Waterloo, Ont., Canada N2L 3G1
[b] Department of Chemistry, University of Waterloo, Waterloo, Ont., Canada N2L 3G1

Received 26 September 2006; in revised form 17 October 2006
Available online 25 October 2006

Abstract

The $\tilde{D}^2\Sigma^+$ state of CaOH was investigated using optical–optical double resonance spectroscopy. A combined least-squares fit of the $\tilde{D}^2\Sigma^+$–$\tilde{A}^2\Pi$ double resonance transition data along with $\tilde{A}^2\Pi$–$\tilde{X}^2\Sigma^+$ optical transition data and the millimeter-wave pure rotational data of the $\tilde{X}^2\Sigma^+$ state was performed using an effective Hamiltonian. The spin–rotation constant was determined for the $\tilde{D}^2\Sigma^+$ state for the first time. An analysis of these constants showed that the Ca–O bond length and spin–rotation parameter of the $\tilde{D}^2\Sigma^+$ state have the smallest values of all the observed $^2\Sigma^+$ states of CaOH. This evidence suggests the assignment of the $\tilde{D}^2\Sigma^+$ state as arising from a Ca^+ atomic orbital of mainly $5s\sigma$ character. This atomic orbital assignment was shown to be consistent with both previous work on CaF and recent theoretical calculations on CaOH.

Keywords: CaOH; Calcium-bearing molecules; Optical–optical double resonance; Alkaline-earth metal–ligand bonding

1. Introduction

Recently, we have been investigating the spectra and structure of alkaline-earth-containing polyatomic molecules. This has included studies of the higher energy states of the metal hydroxides using the technique of optical–optical double resonance spectroscopy (OODR) [1,2]. The higher lying states of these polyatomic molecules are of interest because the molecular structure may vary as the energy of the state increases and the metal–ligand bond becomes more covalent. Also the ordering and atomic orbital character of the electronic states may change with respect to their diatomic counterparts.

A prime candidate for a study of the higher energy states is CaOH. As CaF has already been extensively studied (e.g. [3]), comparisons of the electronic state ordering between these two isoelectronic calcium-containing molecules can easily be made. In addition, preliminary evidence indicates that some of the higher lying states of CaOH may adopt a nonlinear geometry in contrast to the lower lying states in which CaOH has been found to be linear.

The first high-resolution spectroscopic investigation of CaOH was completed by Hilborn and co-workers [4]. In this study, the $\tilde{A}^2\Pi$–$\tilde{X}^2\Sigma^+$ transition was observed and preliminary rotational constants were determined for each state. This work was followed by a more extensive investigation of this transition by Bernath and Brazier [5], in which the molecular parameters were refined. Subsequent studies of the $\tilde{A}^2\Pi$–$\tilde{X}^2\Sigma^+$ transition have probed the vibrational structure of each state using laser-induced fluorescence spectroscopy [6–11]. In addition, the $\tilde{A}^2\Pi$–$\tilde{X}^2\Sigma^+$ transition for the isotopologue CaOD has also been studied [12]. The $\tilde{B}^2\Sigma^+$–$\tilde{X}^2\Sigma^+$ transition has also been observed both at low [13] and high [5,14] resolution. The $\tilde{C}^2\Delta$–$\tilde{X}^2\Sigma^+$ transitions of both CaOH and CaOD have been recorded at high resolution using the technique of laser

* Corresponding author. Present address: Department of Chemistry, University of York, Heslington, York YO10 5DD, UK. Fax: +44 1904 432516.
E-mail address: pfb500@york.ac.uk (P.F. Bernath).
[1] Present address: Department of Chemistry and Biochemistry, Canisius College, Buffalo, NY 14208-1098, USA.

0022-2852/$ - see front matter © 2006 Elsevier Inc. All rights reserved.
doi:10.1016/j.jms.2006.10.009

excitation spectroscopy [15,16]. Pure rotational transitions in the ground state have been recorded by millimeter-wave spectroscopy [17–20] and hyperfine constants arising from the hydrogen nucleus have been determined in the $\tilde{X}^2\Sigma^+$ state using the pump/probe microwave-optical double resonance technique [21]. Finally, the dipole moment of CaOH in the $\tilde{X}^2\Sigma^+$, $\tilde{A}^2\Pi$, and $\tilde{B}^2\Sigma^+$ states has been determined using Stark spectroscopy [22].

The higher energy states of CaOH (>23 000 cm^{-1}) have not been as thoroughly investigated as the lower energy states. Pereira and Levy [23] have used resonance-enhanced multiphoton ionization and laser-induced fluorescence spectroscopic techniques in a molecular beam source to observe the $\tilde{D}^2\Sigma^+$–$\tilde{X}^2\Sigma^+$, $\tilde{E}^2\Sigma^+$–$\tilde{X}^2\Sigma^+$, and $\tilde{F}^2\Pi$–$\tilde{X}^2\Sigma^+$ transitions of CaOH. From their moderate resolution spectra they were able to determine preliminary rotational constants for the $\tilde{D}^2\Sigma^+$ state. In addition, they observed several vibrational bands for each electronic transition and found extensive activity in the bending mode of the $\tilde{F}^2\Pi$ state, indicating that CaOH could possess a nonlinear configuration in this state. Finally, the $\tilde{G}^2\Pi$–$\tilde{B}^2\Sigma^+$ transitions of both CaOH and CaOD has been recorded at moderate resolution using OODR spectroscopy [24]. Several vibrational bands were observed and preliminary rotational and vibrational constants were determined for the $\tilde{G}^2\Pi$ state.

In this paper we present the results of our high-resolution study of the $\tilde{D}^2\Sigma^+$–$\tilde{A}^2\Pi$ transition of CaOH using OODR spectroscopy. For the $\tilde{D}^2\Sigma^+$ state, rotational and fine structure constants have been determined. Using these parameters the molecular structure and the orbital character for the $\tilde{D}^2\Sigma^+$ state have been derived. In addition, a comparison of the energy state ordering between CaOH and CaF will be presented.

2. Experimental

Gas-phase CaOH was produced in a Broida-type oven by resistively heating calcium metal in a graphite crucible until sublimation occurred. The metal vapor was then carried into the reaction region above the crucible by a flow of argon carrier gas (~1–2 Torr). The calcium atoms were reacted with a few mTorr of concentrated hydrogen peroxide, which was introduced through a perforated stainless steel ring located above the crucible. This reaction produced a chemiluminescent flame of CaOH molecules.

The $\tilde{D}^2\Sigma^+$–$\tilde{A}^2\Pi$ transition of CaOH was studied using OODR spectroscopy [1]. A linear cavity dye laser (Kiton red laser dye, output power ~1 W, bandwidth ~1 cm^{-1}) was used to excite the $\tilde{A}^2\Pi$–$\tilde{X}^2\Sigma^+$ transition. The excitation wavelength was systematically varied in order to populate specific groups of rotational levels in the intermediate $\tilde{A}^2\Pi$ state. For example, in order to populate the maximum number of rotational levels, the pump laser was tuned to the band heads of each spin–orbit component of the $\tilde{A}^2\Pi$–$\tilde{X}^2\Sigma^+$ transition (~15 957 cm^{-1} for the P_{11} and Q_{12} heads and ~16 027 cm^{-1} for the P_{21} and Q_{22} heads). A single mode titanium–sapphire ring laser (probe laser) (bandwidth ~10 MHz) operating in the 750–870 nm range was used to promote the CaOH molecules from the intermediate $\tilde{A}^2\Pi$ state to the $\tilde{D}^2\Sigma^+$ state.

The pump and probe laser beams were directed collinearly into the Broida oven chamber and overlapped in the chemiluminescent flame where the concentration of CaOH was greatest. Care was taken to make sure that the two beams were precisely overlapped to ensure that a maximum number of molecules were excited to the $\tilde{D}^2\Sigma^+$ state. As the probe laser wavelength was scanned, UV fluorescence from the $\tilde{D}^2\Sigma^+$ state was detected using a photomultiplier tube (PMT) with a 500 nm blue pass filter. Phase-sensitive detection was utilized by amplitude modulating the pump beam with a mechanical chopper and processing the output signal of the PMT with a lock-in amplifier. The combination of the blue pass filter and phase-sensitive detection ensured that the fluorescence signals observed arose only from the OODR experiment.

Typically spectra were recorded in 5 cm^{-1} segments at a scan speed of 30 s per wavenumber and a data sampling interval of 20 MHz. Absorption spectra of heated I_2 were recorded simultaneously. The I_2 lines were used to calibrate the spectra of the $\tilde{D}^2\Sigma^+$–$\tilde{A}^2\Pi$ transition [25].

3. Results and analysis

From the previous work of Pereira and Levy [23], approximate probe laser frequencies for this investigation of the $\tilde{D}^2\Sigma^+$–$\tilde{A}^2\Pi$ transition of CaOH were determined. In Fig. 1, high-resolution spectra for the $\tilde{D}^2\Sigma^+$–$\tilde{A}^2\Pi_{3/2}$ spin–orbit component using two different pump laser wavenumbers are shown. In the upper panel the pump laser wavenumber (16 027 cm^{-1}) corresponds to the $Q_{22}(e,f)$ and $P_{21}(e,e)$ heads in the $\tilde{A}^2\Pi_{3/2}$–$\tilde{X}^2\Sigma^+$ transition, which results in e parity levels in the intermediate state being predominantly populated. As a result the observed branches in the upper panel are $P_{12}(e,e)$, $R_{12}(e,e)$ and $Q_{22}(f,e)$. The pattern of two intense regions of lines for the $P_{12}(e,e)$ branch is a result of the distribution of J levels populated by the pump laser. In the lower panel, the pump laser wavenumber (16 034 cm^{-1}) corresponds to the $R_{22}(f,f)$ branch in the $\tilde{A}^2\Pi_{3/2}$–$\tilde{X}^2\Sigma^+$ transition. The change in pump laser frequency results in fewer lines being observed because the pump laser is no longer tuned to a band head. In addition, because the f parity levels in the $\tilde{A}^2\Pi_{3/2}$ state are now being predominantly populated, the observed features in the $\tilde{D}^2\Sigma^+$–$\tilde{A}^2\Pi_{3/2}$ transition are the $Q_{12}(e,f)$, $P_{22}(f,f)$, and $R_{22}(f,f)$ branches. Finally, the lines located at ~12 110 cm^{-1} belong to high J values of the $P_{12}(e,e)$ branch, which are present as a result of the pump laser additionally exciting high J lines in the $Q_{22}(e,f)$ and $P_{21}(e,e)$ branches of the $\tilde{A}^2\Pi$–$\tilde{X}^2\Sigma^+$ transition.

Fig. 2 contains a collection of spectra recorded for the $\tilde{D}^2\Sigma^+$–$\tilde{A}^2\Pi_{3/2}$ transition by systematically varying the pump laser wavenumber. By increasing the laser by one wavenumber at a time, and scanning the probe laser over the same spectral region, the $Q_{12}(e,f)$ and $P_{22}(f,f)$ branches

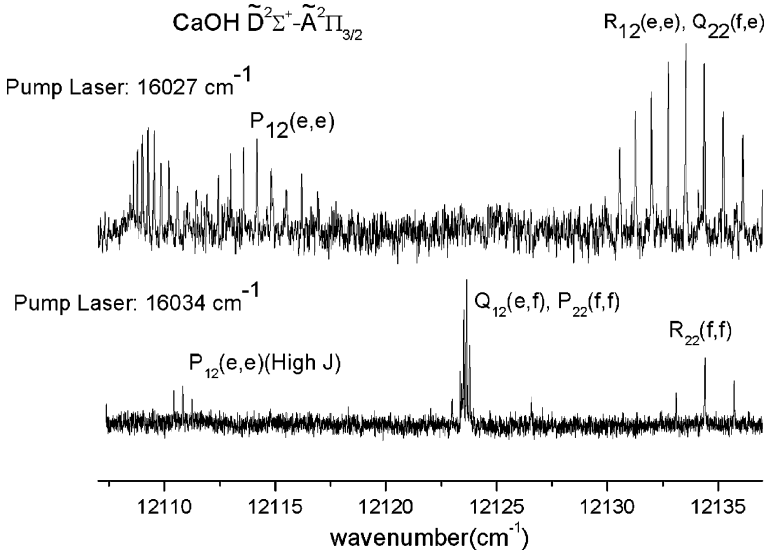

Fig. 1. Optical–optical double resonance spectra of the $\tilde{D}^2\Sigma^+$–$\tilde{A}^2\Pi_{3/2}$ transition of CaOH. In the top panel, the pump laser wavenumber of 16027 cm^{-1} corresponds to the $Q_{22}(e,f)$ and $P_{21}(e,e)$ band heads in the $\tilde{A}^2\Pi_{3/2}$–$\tilde{X}^2\Sigma^+$ transition. As a result levels of e parity are primarily populated in the intermediate state and only lines belonging to the $P_{12}(e,e)$, $R_{12}(e,e)$ and $Q_{22}(f,e)$ branches of the $\tilde{D}^2\Sigma^+$–$\tilde{A}^2\Pi_{3/2}$ transition are observed. In the bottom panel the pump laser wavenumber has been changed to 16034 cm^{-1}, which corresponds to the $R_{22}(f,f)$ branch of the $\tilde{A}^2\Pi_{3/2}$–$\tilde{X}^2\Sigma^+$ transition. Fewer lines are present in this spectrum as compared to the top panel, however, the majority of lines now arise from branches in which the lower energy levels have f parity.

could be tracked from low J to high J in and out of the band head. The resulting spectra facilitated the rotational assignment of these branches. In addition, at high J values a splitting between the $Q_{12}(e,f)$ and $P_{22}(f,f)$ branches was resolved, which is a result of the spin–rotation splitting in the $\tilde{D}^2\Sigma^+$ state.

Rotational assignments for $\tilde{D}^2\Sigma^+$–$\tilde{A}^2\Pi_{3/2}$ transition were made using lower state combination differences in the $\tilde{A}^2\Pi$ state [4,5]. In total 205 rotational lines from 10 of the 12 branches from both spin orbit components of the $\tilde{D}^2\Sigma^+$–$\tilde{A}^2\Pi$ transition of CaOH were assigned. The measured lines are available as supplemental material from the journal. A least-squares fit of the measured data to the Hunds's case (b) $^2\Sigma^+$–Hund's case (a) $^2\Pi$ ($\hat{N}^2$) Hamiltonian of Brown [26] was performed. To minimize the uncertainties and determine the molecular parameters of the $\tilde{D}^2\Sigma^+$ state more precisely, the pure rotational [17] and $\tilde{A}^2\Pi$–$\tilde{X}^2\Sigma^+$ (0_0^0) transition data [4,5] were included in the fit. Each data set was weighted according to its experimental uncertainty. The estimated uncertainty for the pure rotational data was 1.7×10^{-6} cm^{-1}. For the $\tilde{D}^2\Sigma^+$–$\tilde{A}^2\Pi$ and $\tilde{A}^2\Pi$–$\tilde{X}^2\Sigma^+$ (0_0^0) [5] transitions the uncertainties were estimated as 0.005 cm^{-1} for clean lines and 0.02 cm^{-1} for overlapped lines. The $\tilde{A}^2\Pi$–$\tilde{X}^2\Sigma^+$ (0_0^0) transition data of Hilborn et al. [4] was weighted to 0.02 cm^{-1}. The spectroscopic parameters determined in the fit are listed in Table 1. The standard deviation of the fit was ~0.004 cm^{-1} consistent with the experimental uncertainty. For the $\tilde{D}^2\Sigma^+$ state, the band origin, T_{00}, (28156.2006 cm^{-1}) and rotational constant, B, (0.3590134 cm^{-1}) are similar in value, but more precisely determined, than in the previous work ($T_{00}=28\,153$ cm^{-1}, $B=0.36445$ cm^{-1}) [23]. In addition, the centrifugal distortion constant, D, and the spin–rotation parameter, γ, were determined for the first time.

4. Discussion

The spin–rotation constant in the $\tilde{D}^2\Sigma^+$ state of CaOH was found to be positive and very small ($\gamma=8.47\times10^{-4}$ cm^{-1}). The value of γ in the $\tilde{D}^2\Sigma^+$ state can be rationalized by considering the second-order contributions to this parameter arising from spin–orbit coupling. By invoking the unique perturber and pure precession relationships, the following expression for γ can be derived [27]:

$$\gamma=\frac{2A_{SO}B\ell(\ell+1)}{E(^2\Pi)-E(\tilde{D}^2\Sigma^+)}, \tag{1}$$

where B is the rotational constant, A_{SO} is the spin–orbit constant, ℓ is the atomic orbital angular momentum of the $^2\Pi$ state, and E is the state energy. Using the value of γ in the $\tilde{D}^2\Sigma^+$ state, the location of the perturbing $^2\Pi$ state can be estimated. Assuming the perturbing state has molecular parameters similar to the $\tilde{A}^2\Pi$ state ($A_{SO}\sim67$ cm^{-1}, $B\sim0.34$ cm^{-1} and $\ell=1$) [5], the perturbing $^2\Pi$ state would lie approximately 100 000 cm^{-1} above the $\tilde{D}^2\Sigma^+$ state. This separation is unreasonable as two $^2\Pi$ states have already been identified within 10 000 cm^{-1} of the $\tilde{D}^2\Sigma^+$ state ($\tilde{F}^2\Pi$ (30 215 cm^{-1}) [23] and $\tilde{G}^2\Pi$ (36230.2 cm^{-1}) [24]).

A more plausible explanation for the small magnitude of the spin–rotation parameter in $\tilde{D}^2\Sigma^+$ state is that like the $\tilde{X}^2\Sigma^+(4s\sigma)$ state, it is arises from a Ca^+ atomic orbital of predominantly $s\sigma$ character ($5s\sigma$). Electronic states arising from atomic orbitals of $s\sigma$ character do not form a pure precession pair with neighboring $^2\Pi$ states. This explains the similarity in the γ values of the $\tilde{X}^2\Sigma^+$ (1.159647×10^{-3} cm^{-1}) and $\tilde{D}^2\Sigma^+$ (8.47×10^{-4} cm^{-1}) [5] states. In contrast, the $\tilde{B}^2\Sigma^+$ state, which arises from an atomic orbital of

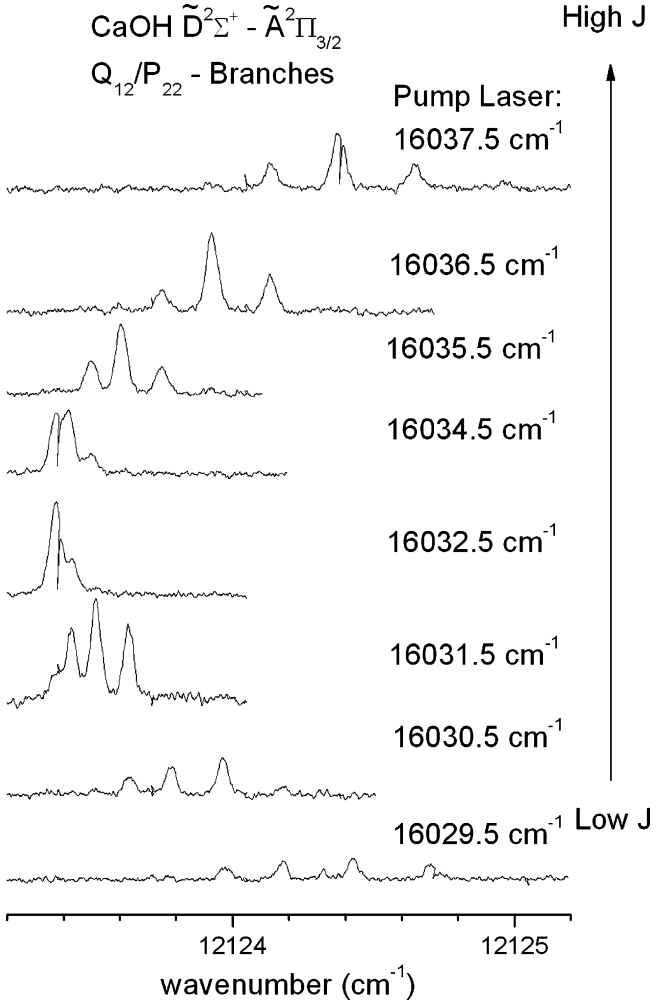

Fig. 2. A series of $\tilde{D}^2\Sigma^+$–$\tilde{A}^2\Pi_{3/2}$ spectra observed at varying pump laser wavenumbers. Overlapped lines belonging to the $Q_{12}(e,f)$ and $P_{22}(f,f)$ branches are tracked in and out of the congested band head region from low J (bottom) to high J (top). At high J, a small splitting between the $Q_{12}(e,f)$ and $P_{22}(f,f)$ branches is present due to the spin–rotation splitting in the $\tilde{D}^2\Sigma^+$ state.

mainly $4p\sigma$ character and forms a unique perturber pair with the $\tilde{A}^2\Pi$ state, has a γ value (-4.3615×10^{-2} cm^{-1}) that is over an order of magnitude larger than the other $^2\Sigma^+$ states.

The rotational data for the $\tilde{D}^2\Sigma^+$ state was successfully modeled using a $^2\Sigma^+$ Hamiltonian, confirming a linear structure for CaOH in this state. Table 2 shows a comparison of the Ca–O and O–H bond lengths for the first vibrational levels of the electronic states of CaOH which have been studied at high resolution. For the $\tilde{B}^2\Sigma^+$, $\tilde{C}^2\Delta$ and $\tilde{D}^2\Sigma^+$ states, rotational constants exist for only one isotopologue thus the O–H bond lengths were fixed to the value obtained for the ground state. The r_0(Ca–O) value in the $\tilde{D}^2\Sigma^+$ state is 3–6% smaller than any other observed state. This is consistent with the assignment of $5s\sigma$ atomic orbital character for the $\tilde{D}^2\Sigma^+$ state as this orbital should be diffuse, allowing the OH^- ligand to approach more closely to the Ca^+ cation, resulting in a shorter Ca–O bond. It should be noted that the assumption that the O–H bond length does not change upon excitation to the $\tilde{D}^2\Sigma^+$ state ignores the possibility of large amplitude bending motion. This motion would effectively reduce the O–H bond length and increase the observed B value for the $\tilde{D}^2\Sigma^+$ state. In order to derive a more reliable molecular structure data for CaOD is needed.

In a recent publication, Taylor et al. [28] used the effective valence shell Hamiltonian method to examine the ground and excited states of CaOH. For the $\tilde{D}^2\Sigma^+$ state, they determined values for the band origin (28 027 cm^{-1}) and Ca–O bond length (1.926 Å). Our experimental observations ($T_{00}=28156.20007$ cm^{-1}, r_0(Ca–O) = 1.912 Å) agree well and confirm these theoretical predictions. In addition, Taylor et al. has also suggested that the $\tilde{D}^2\Sigma^+$ state arises from an atomic orbital which is slightly diffuse and as a result the $\tilde{D}^2\Sigma^+$ state will have the shortest Ca–O separation. These suggestions are consistent with our assignment of predominantly $5s\sigma$ atomic orbital character for the $\tilde{D}^2\Sigma^+$ state.

The spectroscopic parameters observed for the $\tilde{D}^2\Sigma^+$ state of CaOH are also consistent with the previous work on the $\tilde{D}^2\Sigma^+$ state of CaF [29]. First, the spin–rotation constants of the $\tilde{D}^2\Sigma^+$ states of these two molecules (γ(CaOH) = 8.47×10^{-4} cm^{-1}, γ(CaF) = 3×10^{-4} cm^{-1}) are similar in magnitude and sign. Second, as for CaOH, the $\tilde{D}^2\Sigma^+$ state

Table 1
Spectroscopic constants (in cm^{-1}) for CaOH[a,b]

Constant	$\tilde{X}^2\Sigma^+(000)$	$\tilde{A}^2\Pi(000)$	$\tilde{D}^2\Sigma^+(000)$
T	0.0	15997.77579(64)	28156.20008(99)
B	0.334334107(32)	0.3412272(15)	0.3590164(26)
D	$3.86000(86)\times10^{-7}$	$3.8960(65)\times10^{-7}$	$3.995(14)\times10^{-7}$
γ	$1.15957(51)\times10^{-3}$		$8.47(35)\times10^{-4}$
A		66.81480(89)	
A_D		$-1.741(10)\times10^{-4}$	
p		$-4.3064(71)\times10^{-2}$	
q		$-3.447(24)\times10^{-6}$	

[a] Values in parentheses are 1σ standard deviations, in units of the last significant digits.
[b] Combined fit of the $\tilde{D}^2\Sigma^+$–$\tilde{A}^2\Pi$ transition data, $\tilde{X}^2\Sigma^+$ state millimeter-wave data [18], and the $\tilde{A}^2\Pi$–$\tilde{X}^2\Sigma^+$ transition data [10,11].

Table 2
Bond lengths (Å) for CaOH

	$\tilde{X}^2\Sigma^+$[a]	$\tilde{A}^2\Pi$[b]	$\tilde{B}^2\Sigma^+$[c]	$\tilde{C}^2\Delta$[d]	$\tilde{D}^2\Sigma^+$[e]
r_0(CaO)	1.985	1.964	1.969	2.019	1.912
r_0(OH)	0.921	0.920	0.921	0.921	0.921

[a] Determined from the millimeter-wave data of CaOH [18] and CaOD [20].
[b] Determined from the optical data of CaOH [10,11] and CaOD [24].
[c] Determined from the optical data of CaOH [11] and a fixed r_0(OH) of 0.921 Å.
[d] Determined from the optical data of CaOD [27] and a fixed r_0(OH) of 0.921 Å.
[e] Determined from the optical data of CaOH [this work] and a fixed r_0(OH) of 0.921 Å.

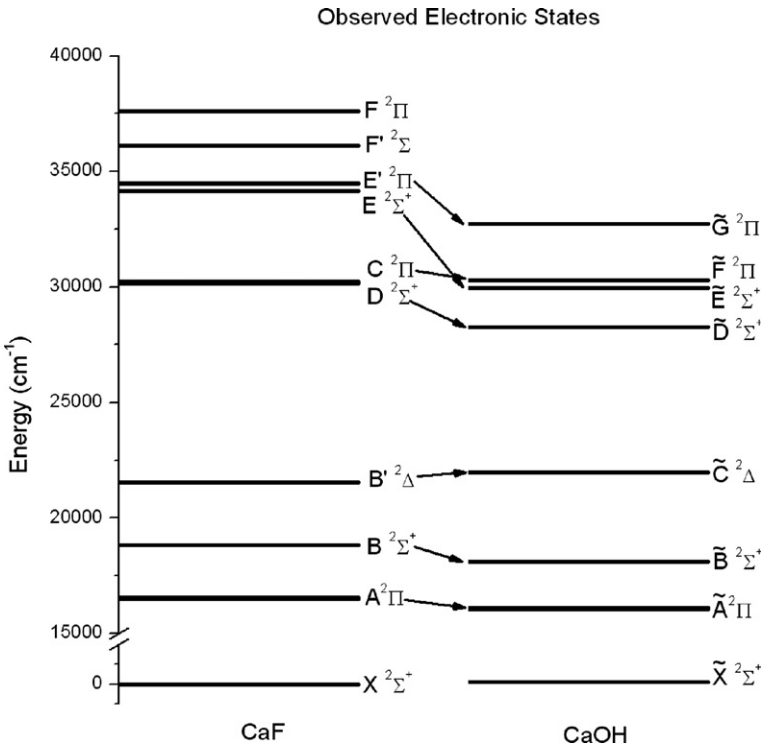

Fig. 3. An energy level diagram correlating the observed electronic states of CaF with those of CaOH. In general, substitution of OH^- for F^- results in a lowering of the energy of the observed states, except for the $^2\Delta$ state. The $^2\Sigma^+$ states appear to be the most affected by the ligand change and the $\tilde{D}^2\Sigma^+$ state of CaOH is more isolated as compared to its counterpart in CaF.

of CaF was found to have the shortest Ca-ligand separation (r_0(Ca–F) = 1.893 Å) of the ground and first four excited electronic states. The similarity between the molecular parameters for the $\tilde{D}^2\Sigma^+$ state of each molecule suggests that the atomic orbital character of this state is not changing significantly as the ligand varies. For each molecule, the dominant orbital character of the $\tilde{D}^2\Sigma^+$ state is $5s\sigma$.

While the orbital character of the observed electronic states of CaF and CaOH generally appears invariant, the electronic energy state ordering does not. Fig. 3 shows a comparison of the observed electronic states of CaOH with CaF. This diagram illustrates that the electronic states have reordered slightly from halide to hydroxide ligand. With the exception of the $^2\Delta$ state, the electronic states have shifted to slightly lower energies in CaOH as compared to CaF. In addition, the $^2\Sigma^+$ states seem to have been the most affected by the change in ligand. Specifically, the $\tilde{D}^2\Sigma^+$ state has moved such that it is more isolated in CaOH. This increased isolation, which does not affect the molecular parameters of CaOH as compared to CaF, is further evidence that the $\tilde{D}^2\Sigma^+$ arises from an atomic orbital which does not interact with neighboring electronic states ($5s\sigma$). For example, as previously mentioned, there is no significant change in the observed spin rotation constants of CaOH and CaF despite the neighboring $^2\Pi$ states being closer in energy to the $\tilde{D}^2\Sigma^+$ state of CaF. Further high-resolution investigations of the other higher lying states of CaOH are needed to see if the apparent invariance of atomic orbital character with ligand change holds as the energies of the states increase.

5. Conclusion

Using the technique of optical–optical double resonance spectroscopy, a high-resolution spectrum of the $\tilde{D}^2\Sigma^+$–$\tilde{A}^2\Pi$ transition of CaOH was recorded for the first time. Rotational and fine structure parameters were determined for the $\tilde{D}^2\Sigma^+$ state from a rotational analysis of the data. Small values for the Ca–O separation and the spin rotation constant in the $\tilde{D}^2\Sigma^+$ state are consistent with predominant $5s\sigma$ orbital character for the $\tilde{D}^2\Sigma^+$ state of CaOH. This atomic orbital assignment is in agreement with previous work on CaF [29] and recent theoretical calculations on CaOH [28]. Finally, a comparison of the electronic state energy ordering of CaOH and CaF shows that the substitution of OH^- for F^- causes the electronic states to shift to lower energy but does not significantly affect the atomic orbital character of the $\tilde{D}^2\Sigma^+$ state.

Acknowledgment

Financial support for this work was provided by the Natural Sciences and Engineering Research Council (NSERC) of Canada.

Appendix A. Supplementary data

Supplementary data for this article are available on ScienceDirect (www.sciencedirect.com) and as part of the

Ohio State University Molecular Spectroscopy Archives (http://msa.lib.ohio-state.edu/jmsa_hp.htm).

References

[1] J.-G. Wang, P.M. Sheridan, M.J. Dick, P.F. Bernath, J. Mol. Spectrosc. 236 (2006) 21–28.
[2] S. Yu, J.-G. Wang, P.M. Sheridan, M.J. Dick, P.F. Bernath, J. Mol. Spectrosc. 240 (2006) 14–19.
[3] J.M. Berg, J.E. Murphy, N.A. Harris, R.W. Field, Phys. Rev. A 48 (1993) 3012–3029.
[4] R.C. Hilborn, Z. Qingshi, D.O. Harris, J. Mol. Spectrosc. 97 (1983) 73–91.
[5] P.F. Bernath, C.R. Brazier, Astrophys. J. 288 (1985) 373–376.
[6] J.A. Coxon, M. Li, P.L. Presunka, J. Mol. Spectrosc. 150 (1991) 33–45.
[7] J.A. Coxon, M. Li, P.L. Presunka, Mol. Phys. 76 (1992) 1463–1476.
[8] M. Li, J.A. Coxon, J. Chem. Phys. 97 (1992) 8961–8969.
[9] J.A. Coxon, M. Li, P.L. Presunka, J. Mol. Spectrosc. 164 (1994) 118–128.
[10] M. Li, J.A. Coxon, J. Chem. Phys. 102 (1995) 2663–2674.
[11] M. Li, J.A. Coxon, J. Chem. Phys. 104 (1996) 4961–4977.
[12] M. Li, J.A. Coxon, Can. J. Phys. 72 (1994) 1200–1205.
[13] R.F. Wormsbecher, M. Trkula, C. Martner, R.E. Penn, D.O. Harris, J. Mol. Spectrosc. 97 (1993) 29–36.
[14] P.F. Bernath, S. Kinsey-Nielsen, Chem. Phys. Lett. 105 (1984) 663–666.
[15] C.N. Jarman, P.F. Bernath, J. Chem. Phys. 97 (1992) 1711–1718.
[16] Z.J. Jakubek, R.W. Field, J. Chem. Phys. 98 (1993) 6574–6575.
[17] L.M. Ziurys, W.L. Barclay Jr., M.A. Anderson, Astrophys. J. 384 (1992) L63–L66.
[18] D.A. Fletcher, M.A. Anderson, W.L. Barclay Jr., L.M. Ziurys, J. Chem. Phys. 102 (1995) 4334–4339.
[19] B.P. Nuccio, A.J. Apponi, L.M. Ziurys, J. Chem. Phys. 103 (1995) 9193–9199.
[20] L.M. Ziurys, D.A. Fletcher, M.A. Anderson, W.L. Barclay Jr., Astrophys. J. Suppl. Ser. 102 (1996) 425–434.
[21] C.T. Scurlock, D.A. Fletcher, T.C. Steimle, J. Mol. Spectrosc. 159 (1993) 350–356.
[22] T.C. Steimle, D.A. Fletcher, K.Y. Jung, C.T. Scurlock, J. Chem. Phys. 96 (1992) 2556–2564.
[23] R. Pereira, D.H. Levy, J. Chem. Phys. 105 (1996) 9733–9739.
[24] R.A. Hailey, C. Jarman, P.F. Bernath, J. Chem. Phys. 107 (1997) 669–670.
[25] S. Gerstenkorn, J. Verges, J. Chevillard, ''Atlas du Spectre d'Absorption de la Molecule d'Iode'' Laboratoire Aimé-Cotton, CNRS II 91405, Orsay, France, 1982.
[26] J.M. Brown, E.A. Colbourn, J.K.G. Watson, F.D. Wayne, J. Mol. Spectrosc. 74 (1979) 294–318.
[27] H. Lefebvre-Brion, R.W. Field, The Spectra and Dynamics of Diatomic Molecules, Elsevier, Amsterdam, 2004.
[28] C.M. Taylor, R.K. Chaudhuri, K.F. Freed, J. Chem. Phys. 122 (2005) 044317-1–044317-13.
[29] C.M. Gittins, N.A. Harris, R.W. Field, J. Vergès, C. Effantin, A. Bernard, J. D'Incan, W.E. Ernst, P. Bundgen, B. Engels, J. Mol. Spectrosc. 161 (1993) 303–311.